

NUMERICAL SIMULATION OF RADIATIVE TRANSFER IN HIGH TEMPERATURE POROUS MEDIA WITH A NULL-COLLISION MONTE CARLO METHOD

P.F.B. Sousa, priscila@mecanica.ufu.br

Federal University of Uberlândia- UFU, School of Mechanical Engineering – FEMEC, Campus Santa Mônica, Av. João Naves de Ávila, 2121, CEP 38408-100, Uberlândia, M.G., Brazil.

M. Roger, maxime.roger@insa-lyon.fr

A. Delmas, agnes.delmas@insa-lyon.fr

Université de Lyon, INSA de Lyon, CETHIL UMR5008, F-69621 Villeurbanne, France

Abstract. Many materials have a heterogeneous structure due to their use and function in various industrial applications. Radiative transfer has a relevant impact in such media because of this structure. For instance, porous or fibrous ceramics used as thermal barrier coatings in the spatial field or as protection of dawn of gas turbines constitute a participating media for radiative transfer. Modeling radiative transfer in heterogeneous media requires generally a homogenization model for the radiative properties. In those approaches, equivalent homogeneous radiative properties (such as the absorption and scattering coefficients or the phase function parameters) are used to estimate radiative transfer. One of the main strengths of the Monte Carlo - Null Collision algorithm presented in this work is its ability to predict radiative transfer in heterogeneous media without homogenization model, since a statistical approach is used for the treatments of the heterogeneities. A numerical code based on this algorithm has been developed. It solves the Radiative Transfer Equation (RTE) in a heterogeneous emitting, absorbing and scattering material, and the Lorenz-Mie theory is used for calculating the radiative properties of the heterogeneities (pores, fibres or particles). Radiative emission measurement have been performed on an experimental set-up developed for high-temperature infrared spectrometry (FTIR) emission measurements. The comparison between the predicted and measured emission for a porous alumina sample (Al_2O_3) at 820K is presented in this work.

Keywords: Radiative transfer model, heterogeneous media, Monte Carlo, Null Collision, spectrometry

1. INTRODUCTION

The prediction of radiative transfer in heterogeneous materials, such as ceramics, foams, porous and fibrous media, is today an active research field (Howell, 2010 and Sacadura, 2011). This issue is important for various industrial applications, such as space, aviation, automobile, solar energy, where the characterization of new materials at high-temperature is critical. In high-temperature processes, radiative transfer has a strong impact on the mechanical properties of materials, and therefore on its performance, which can be very critical in industrial applications such as thermal barrier protections (Lefoll et al., 2012). A better understanding of radiative transfer will lead to a better prediction of the temperature which is strongly requested for the design of the structure, for a better knowledge of the thermo-mechanical properties, and for optimizing these properties in order to improve the performance of the materials.

Heat transfer in heterogeneous media is generally approached with homogenization models. The heterogeneous media are modeled with an equivalent homogeneous media with equivalent homogeneous radiative properties, such as the absorption and scattering coefficients, and the phase function which depends on the particular structure and composition of the real media. In radiative transfer, homogenization models have been proposed in Taine et al.(2010); Zarrouati et al. (2015) and Petrash et al. (2011). The homogenization model may be different than the classical radiative transfer models such as the radiative transfer equation (RTE), and for instance the Beer exponential attenuation due to absorption or scattering may not be valid if homogenization approaches are used (Taine et al., 2010).

The approach proposed in this work is distinct from the work proposed in the literature since no homogenization model is used. The Monte Carlo null-collision algorithm is applied for the simulation of radiative transfer in the heterogeneous material. This meshless algorithm has been recently introduced for radiative transfer in Galtier et al. (2013) and Galtier et al. (2016) . It consists in introducing pure forward scattering events in the Monte Carlo algorithm. Those new events have no influence on radiative transfer but allow to bypass the classical difficulties linked to the integration of the optical thickness along the optical path when the propagation medium is not homogeneous (Galtier et al., 2013). Therefore, based on a statistical approach, radiative transfer is modeled directly at the local scale of the heterogeneities using the Mie theory to determine the radiative properties, and the RTE to treat radiative transfer inside the materials.

In this study, the approach proposed to simulate radiative transfer is detailed, and tested in a porous medium (alumina) at high-temperature. The numerical results are compared to experimental measurements realized on an experimental set-up for high-temperature radiative emission measurements (Galtier et al. 2016). In the next sections, the

radiative transfer models and the Monte Carlo algorithm used in this work are detailed. Then, the experimental bench is briefly described. Finally, validation results are discussed before conclusion.

2. RADIATIVE TRANSFER SIMULATIONS IN HETEROGENEOUS MEDIA BASED ON A MONTE CARLO NULL-COLLISION APPROACH

The Monte Carlo - Null Collision algorithm developed in this work allows to estimate radiative transfer inside a porous or fibrous materials without using an homogenization model. First, the basic principle of the Monte Carlo method in radiative transfer is introduced in homogeneous media, and then the extension of this approach to heterogeneous media with the null-collision algorithm is presented. The radiative properties such as the absorption coefficient and the scattering coefficient, as well as the phase function are calculated from the Mie theory. The input data needed for the calculations are the optical properties (refractive index) which are measurements data provided by the CEMTHI Orléans. Finally, the overall algorithm for the simulation of radiative transfer in heterogeneous materials is detailed

2.1 Models

The radiative transfer equation (RTE) is solved in this work. It can be written as:

$$\vec{u} \vec{\nabla} I_\nu(\vec{x}, \vec{u}) = - \left(k_{s,\nu}(\vec{x}) + k_{a,\nu}(\vec{x}) \right) I_\nu(\vec{x}, \vec{u}) + k_{a,\nu}(\vec{x}) I_{b,\nu}(\vec{x}) + k_{s,\nu}(\vec{x}) \int_{4\pi} p_\nu(\vec{u}/\vec{u}') I_\nu(\vec{x}, \vec{u}') d\vec{u}' \quad (1)$$

where $I_\nu(\vec{x}, \vec{u})$ is the radiative intensity at position \vec{x} , in direction \vec{u} and frequency ν ; $I_{b,\nu}(\vec{x})$ is the blackbody intensity at \vec{x} and ν ; $k_{a,\nu}(\vec{x})$ and $k_{s,\nu}(\vec{x})$ are the absorption and scattering coefficients, respectively; $p_\nu(\vec{u}/\vec{u}')$ is the normalized scattering phase function.

The radiative properties ($k_{a,\nu}(\vec{x})$, $k_{s,\nu}(\vec{x})$ and $p_\nu(\vec{u}/\vec{u}')$) are calculated from the Mie theory. Consequently the heterogeneities are assumed to be spherical (such as spherical particle or pores) or to be infinite cylinder (such as fibers) with those models in this work.

2.2 Principle of the Monte Carlo method for radiative transfer in homogeneous medium

The Monte Carlo method (MCM) is a statistical method for estimating integrals such as:

$$I = \int_D f(\mathbf{x}) d\mathbf{x} \quad (2)$$

where D is a multidimensional domain, and $f(\mathbf{x})$ any function of the multidimensional variable \mathbf{x} . In the Monte Carlo method, a probability density function $p_x(\mathbf{x})$ (positive and normalized in D) is introduced and Eq. (2) is rewritten as,

$$I = \int_D p_x(\mathbf{x}) \frac{f(\mathbf{x})}{p_x(\mathbf{x})} d\mathbf{x} = \int_D p_x(\mathbf{x}) w(\mathbf{x}) d\mathbf{x} \quad (3)$$

where $w(\mathbf{x})$ is called the Monte Carlo weight. Then, the integral is estimated as:

$$I \cong \tilde{I} = \frac{1}{N} \sum_{i=1}^N w(\mathbf{x}_i) \quad (4)$$

where $\{\mathbf{x}_i\}_{i=1,N}$ are N independent realizations of the random variable \mathbf{X} according to $p_x(\mathbf{x})$. The statistical uncertainty (an evaluation of the standard deviation of the estimator) can also be estimated according to:

$$\tilde{\sigma}_N = \frac{1}{\sqrt{N-1}} \sqrt{\left(\frac{1}{N} \sum_{i=1}^N w(\mathbf{x}_i)^2 \right) - \tilde{I}^2} \quad (5)$$

For the simulation of radiative transfer, the radiative transfer equation (RTE), Eq.(1), is solved in its integral form with the MCM :

$$I_\nu(\vec{x}, \vec{u}) = I_\nu(\vec{x}, \vec{u}) \exp\left(-\int_0^{l_w} (k_{a,\nu}(l) + k_{s,\nu}(l)) dl\right) + \int_0^{l_w} \exp\left(-\int_0^l [k_{a,\nu}(l) + k_{s,\nu}(l)] dl\right) \left[k_{a,\nu}(\vec{x}_1) I_{b,\nu}(\vec{x}_1) + k_{s,\nu}(\vec{x}_1) \int_{4\pi} p(\vec{u}/\vec{u}_1) I_\nu(\vec{x}_1, \vec{u}_1) d\vec{u}_1 \right] \quad (6)$$

where $l_w = \|\vec{x} - \vec{x}_w\|$ is the distance between the current position \vec{x} and a position at the boundary of the system \vec{x}_w (see Figure 1). \vec{x}_1 is the first collision position defined as $\vec{x}_1 = \vec{x} - l_1 \vec{u}$.

Considering an homogeneous medium ($k_{a,v}$ and $k_{s,v}$ does not depend anymore on the position) the RTE (Eq. (6)) can be rewritten as:

$$I_v(\vec{x}, \vec{u}) = \int_0^\infty (k_{a,v} + k_{s,v}) \exp(-(k_{a,v} + k_{s,v})l_1) dl_1 \cdot \left\{ H(l_1 - l_w) \cdot I_v(\vec{x}_w, \vec{u}) + H(l_w - l_1) \cdot \left[\frac{k_{a,v}}{k_{a,v} + k_{s,v}} I_{b,v}(\vec{x}_1) + \frac{k_{s,v}}{k_{a,v} + k_{s,v}} \int_{4\pi} p(\vec{u}/\vec{u}_1) I_v(\vec{x}_1, \vec{u}_1) d\vec{u}_1 \right] \right\} \quad (7)$$

where $H(x)$ is the Heaviside step function.

Figure 2 shows schematically an example of optical path that illustrate the notation used in equation (6) and (7).

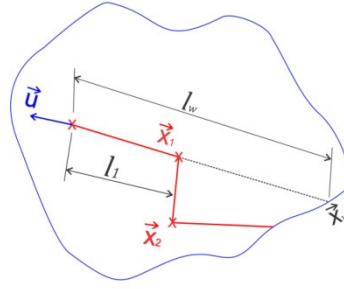


Figure 2. Optical photon path

Eq. (7) can be rewritten in the following form from which the Monte Carlo algorithm can be deduced:

$$I_v(\vec{x}, \vec{u}) = \int_0^\infty P_l(l_1) dl_1 \cdot \left\{ H(l_1 - l_w) \cdot I_v(\vec{x}_w, \vec{u}) + H(l_w - l_1) \cdot \left[P_e I_{b,v}(\vec{x}_1) + P_s \int_{4\pi} p(\vec{u}/\vec{u}_1) I_v(\vec{x}_1, \vec{u}_1) d\vec{u}_1 \right] \right\} \quad (8)$$

where H is the Heaviside step function: $H(x)=1$ if $x > 0$, $H(x)=0$ if $x < 0$, and:

- $P_l(l_1) = k \cdot \exp(-k \cdot l_1)$, with $k = k_{a,v} + k_{s,v}$, is the probability density function (pdf) that an emission or a scattering event occurs at a position \vec{x}_1 , and $l_1 = \|\vec{x}_1 - \vec{x}\|$.
- $H(l_1 - l_w)$ formalize the case where \vec{x}_1 is out of the considered domain. If $l_1 > l_w$, then $H(l_1 - l_w) = 1$, then the radiative intensity at the boundary position \vec{x}_w is considered. $H(l_w - l_1)$ formalize the case where \vec{x}_1 is inside the domain. If a collision occurs, $P_e = \frac{k_{a,v}}{k_{a,v} + k_{s,v}}$ represents the probability that the collision is an emission. $P_s = \frac{k_{s,v}}{k_{a,v} + k_{s,v}} = 1 - P_e$ (also called the scattering albedo) represents the probability that the collision is a scattering event.
- When a scattering event occurs, $p(\vec{u}/\vec{u}_1)$ the normalized phase function represents the pdf that the scattered direction is \vec{u} if the incident direction is \vec{u}_1 .

From this Eq. (8), the following Monte Carlo algorithm is deduced:

- 1 - A loop over the Nth optical path is started; $i=0$.
- 2 - New optical path $i=i+1$; if $i > N$, go to point 5, else $j=0$; $\vec{u}_0 = \vec{u}$; $\vec{x}_0 = \vec{x}$
- 3 - $j=j+1$, Random generation of a path length l_j according to $P_{l_j}(l_j)$
- 4 - $\vec{x}_j = \vec{x}_{j-1} - l_j \cdot \vec{u}_{j-1}$. Two scenarios are possible:
 - 4.1 - \vec{x}_j is inside the domain ($l_j < l_w$). Uniform Sampling of $R \in [0,1]$. Two scenarios are possible
 - 4.1.1 - $R < P_e$. Emission event, $w = I_{b,v}(\vec{x}_j)$, return to point 2.
 - 4.1.2 - $R > P_e$. Scattering event, Random generation of direction \vec{u}_j according to $p(\vec{u}_{j-1}/\vec{u}_j)$, return to point 3.
 - 4.2 - \vec{x}_j is outside the domain ($l_j > l_w$), $w = I(\vec{x}_w, \vec{u}_{j-1})$ (Boundary conditions) return to point 2
- 5 - Estimation of $I(\vec{x}, \vec{u}) \cong \frac{1}{N} \sum_{i=1}^N w_i$ and of $\tilde{\sigma}_N$, (see Eq (4))

Figure 3. MCM algorithm

Note that this algorithm is reverse: the photons optical path are generated in a reverse way, from the end of the optical path (at \vec{x}) until the beginning (emission point or boundary point)

2.3 Null-collision Monte Carlo algorithm for heterogeneous materials

2.3.1 Null Collision Algorithm

When heterogeneous media are considered (like porous or fibrous media), the *pdf* $P_1(l)$ becomes:

$$P_1(l) = (k_{a,v}(l) + k_{s,v}(l)) \exp\left(-\int_0^l (k_{a,v}(l) + k_{s,v}(l)) dl\right) \quad (9)$$

Generally, the integral inside the exponential makes the inversion of the cumulative distribution function (cdf) infeasible. In order to avoid this problem, null-collision algorithms have been introduced (Galtier et al., 2013)

It consists in introducing a null collision event characterized by a null-collision coefficient, $k_{n,v}$, so that the modified extinction coefficient $\hat{k}_v = k_{a,v} + k_{s,v} + k_{n,v}$ is constant, and allows to easily invert the *cdf* of $\hat{P}_1 = \hat{k} \exp(-\hat{k}l)$. A null collision correspond to a pure-forward scattering event, and consequently has no influence on the radiative transfer. Equation (8) can be rewritten as:

$$I_v(\vec{x}, \vec{u}) = \int_0^\infty \hat{P}_1(l_1 dl_1 \cdot \{H(l_1 - l_w) \cdot I_v(\vec{x}_w, \vec{u})\} + H(l_w - l_1) \cdot \left[P_e(\vec{x}_1) I_{b,v}(\vec{x}_1) + P_s(\vec{x}_1) \int_{4\pi} p(\vec{u}' / \vec{u}_1) I_v(\vec{x}_1, \vec{u}_1) d\vec{u}_1 + P_n(\vec{x}_1) \int_{4\pi} \delta(\vec{u}' - \vec{u}_1) \cdot I_v(\vec{x}_1, \vec{u}_1) d\vec{u}_1 \right] \quad (10)$$

Equation (10) is strictly identical to the RTE. Now, the emission, scattering and null-collision probabilities are written as:

$$P_e(\vec{x}_1) = \frac{k_{a,v}(\vec{x}_1)}{\hat{k}_v}, \quad P_s(\vec{x}_1) = \frac{k_{s,v}(\vec{x}_1)}{\hat{k}_v} \quad \text{and} \quad P_n(\vec{x}_1) = \frac{\hat{k}_v - k_{a,v}(\vec{x}_1) - k_{s,v}(\vec{x}_1)}{\hat{k}_v} \quad (11)$$

Figure 4 describes the Monte Carlo - Null Collision algorithm:

- 1 - A loop over the Nth optical path is started; $i=0$
- 2 - New optical path $i=i+1$; if $i > N$, go to point 5, else $j=0$; $\vec{u}_0 = \vec{u}$; $\vec{x}_0 = \vec{x}$
- 3 - $j=j+1$, Random generation of a path length l_j according to $\hat{P}_{1j}(l_j)$
- 4 - $\vec{x}_j = \vec{x}_{j-1} - l_j \cdot \vec{u}_{j-1}$. Two scenarios are possible:
 - 4.1 - \vec{x}_j is inside the domain ($l_j < l_w$). Uniform Sampling of $R \in [0,1]$. Three scenarios are possible
 - 4.1.1 - $R < P_e$. Emission event, $w = I_{b,v}(\vec{x}_j)$, return to point 2.
 - 4.1.2 - $P_e < R < P_s$. Scattering event, Random generation of direction \vec{u}_j according to $p(\vec{u}_{j-1}/\vec{u}_j)$, return to point 3.
 - 4.1.3 - $R > P_s$. Null Collision event, return to point 3.
 - 4.2 - \vec{x}_j is outside the domain ($l_j > l_w$). $w_i = I(\vec{x}_{w,j}, \vec{u}_{j-1})$ (Boundary conditions) return to point 2
- 5 - Estimation of $I(\vec{x}, \vec{u}) \cong \frac{1}{N} \sum_{i=1}^N w_i$ and of $\tilde{\sigma}_N$, see Eq (4)

Figure 4. Monte Carlo - Null Collision algorithm

2.3.2. Application to heterogeneous materials

The developed numerical code is able to calculate radiative intensity for a heterogeneous media. The case discussed in this work consists of an absorbing matrix, called medium 1, and randomly dispersed pores, named medium 2 (Fig. 5). In this study, the propagation medium (porous or fibrous), is described statistically thanks to the f_v , volumetric fraction, that is, the porosity of the medium if pores are considered. Indeed, f_v can be seen as the probability that a photon inside the medium is in a pore (medium 2 in Fig. 5). Consequently the probability of the photon to be in the solid matrix in the case of porous media is given by $(1 - f_v)$.

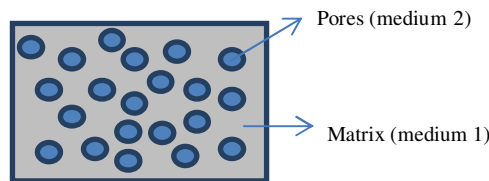


Figure 5. Test case: Al₂O₃ matrix and pores filled with air

Therefore, each time a new position \vec{x}_i has been generated inside the medium, a random number $R_1 \in [0, 1]$ is generated. If $R_1 < f_v$, it means that the position is inside a pore. According to the frequency, and the radius of the pore, the Mie theory is used to determine the local absorption and scattering coefficients $k_{a,v}(\vec{x}_i)$ and $k_{s,v}(\vec{x}_i)$. Finally, another random number R_2 is generated to determine if it is an emission, a scattering or null-collision events.

The proposed algorithm is detailed in Fig. 6:

- 1 - A loop over the N_{th} optical path is started; $i=0$
- 2 - New optical path $i=i+1$; if $i > N$, go to point 5, else $j=0$; $\vec{u}_0 = \vec{u}$; $\vec{x}_0 = \vec{x}$
- 3 - $j=j+1$, Random generation of a length l_j according to $\hat{P}_{lj}(l_j)$
- 4 - $\vec{x}_j = \vec{x}_{j-1} - l_j \cdot \vec{u}_{j-1}$. Two scenarios are possible:
 - 4.1 - \vec{x}_j is inside the domain ($l_j < lw$). Uniform Sampling of $R_1 \in [0,1]$.
 - 4.1.1 - if $R_1 < f_v$, $\vec{x}_j \in$ medium 2 (pore); estimation of $k_{a,v}(\vec{x}_j)$, $k_{s,v}(\vec{x}_j)$ and phase function according to the Lorenz-Mie theory
 - 4.1.2 - if $R_1 > f_v$, $\vec{x}_j \in$ medium 1 (solid matrix); $k_{a,v}(\vec{x}_j) = k_{a,v,1}$, $k_{s,v}(\vec{x}_j) = k_{s,v,1}$
 Uniform sampling of $R_2 \in [0,1]$.
 - 4.1.1.1 - $R_2 < P_e$. Emission event, $w = I_{b,v}(\vec{x}_j)$, return to point 2.
 - 4.1.1.2 - $P_e < R_2 < P_s$. Scattering event, Random generation of direction \vec{u}_j according to $p(\vec{u}_{j-1}/\vec{u}_j)$, return to point 3.
 - 4.1.1.3 - $R_2 > P_s$. Null Collision event, return to point 3.
 - 4.2 - \vec{x}_j is outside the domain ($l_j > lw$). $w_i = I(\vec{x}_w, \vec{u}_{j-1})$ (Boundary conditions) return to point 2
- 5 - Estimation of $I(\vec{x}, \vec{u}) \cong \frac{1}{N} \sum_{i=1}^N w_i$ and of $\bar{\sigma}_N$, see Eq (4)

Figure 6. Monte Carlo - Null Collision algorithm for porous media

This algorithm is therefore able to estimate radiative transfer in pores or fibrous media (if infinite cylinder are assumed) without homogenization.

3. EXPERIMENTAL SET UP

3.1 Experimental set up

An experimental bench dedicated to radiative emission measurements by infrared spectrometry (FTIR) is used at CETHIL (Center of Energy and Thermal Sciences of Lyon-France) laboratory, to characterize radiative properties of ceramics at high temperatures from 800 K to 2000 K. A schematic representation of the experimental set up is shown in Fig. 7. The studied ceramic samples are heated by a CO₂ laser. The original beam is split (beam splitter) in two identical beams that enter the vacuum chamber by ZnSe optical windows and reach both faces of the sample. The surface of the side faces of square samples is 11x11 mm² and the thickness is 2.5 mm.

The emitted spectral radiative heat flux from the sample is measured by a BRUKER FTIR spectrometer in the wavelength range lying from 2μm to 10 μm. Calibrating the test bench with a high temperature PIROX PY25 blackbody leads to radiative intensity spectra. Surface temperatures are measured by pyrometry at the Christiansen frequency.

Table 1: Christiansen wavelength for Alumina

Material	λ_{Chr} [μm]	ϵ_{Chr}	λ range [μm] $\epsilon > 0,99$
Al ₂ O ₃	9.5	0.999	8.7—10.2

Spectrometric measurements are performed only on one face of the sample.

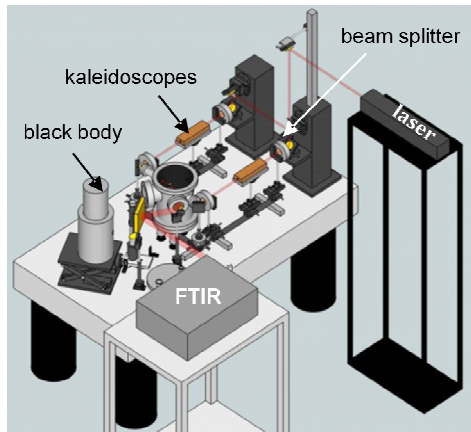


Figure 7. Schematic representation of the bench

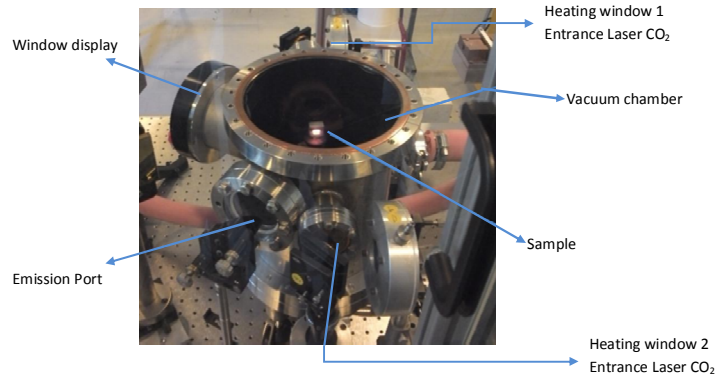


Figure 8. Vacuum chamber equipped with optical windows

3.2 Measured Radiative emission spectra

The first step consists in the determination of the spectral calibration function $H(\sigma, T)$, where σ is the wavenumber, $\sigma(\text{cm}^{-1}) = \frac{10^4}{\lambda(\mu\text{m})}$. Emission spectra $S(\sigma)$ are performed on the blackbody reference for several temperature. The calibration function for a given temperature T is obtained as the ratio of $S(\sigma, T)$ over the Planck emission power at the same temperature $I_{b,\sigma}(T)$. An example of calibration functions is presented in Fig. 9 for temperatures lying between 973K to 1575K. These measurements show that the calibration function is almost independent of temperature. Atmospheric absorption bands are present on the calibration function as radiation propagates in air from the emission window of the vacuum chamber to the detector in the FTIR.

Since the two optical paths, from the sample to the spectrometer, and from the blackbody to the spectrometer are similar, the same calibration function is used to determine the radiative intensity of the sample from emission measurements as follows :

$$I_{\sigma}(T) = \frac{S(\sigma, T)}{H_{\text{cm}}(\sigma, T)} \quad (12)$$

A measured spectral intensity on a sample of alumina is presented in Fig. 10 as an example.

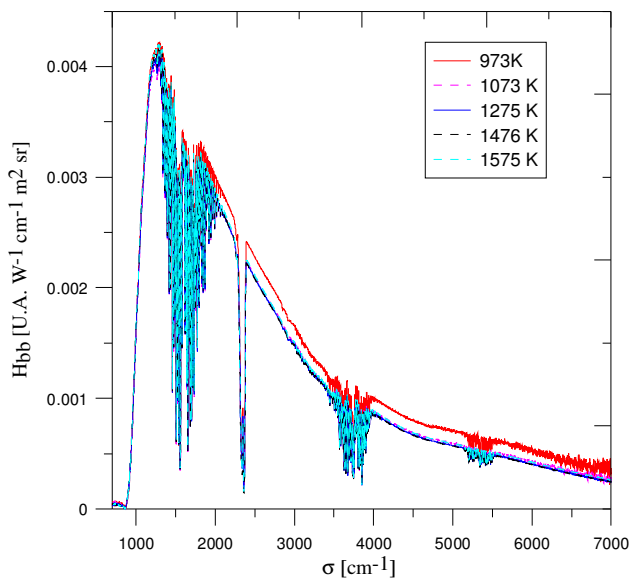


Figure 9. Spectral calibration functions

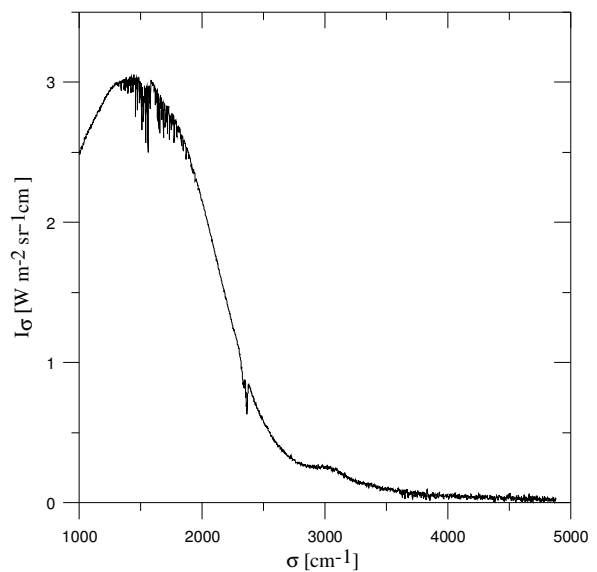


Figure 10. Measured spectral intensity on a Al_2O_3 sample

4. VALIDATION RESULTS

The results presented in this section compare simulation and measurements of the spectral emission factor defined as :

$$\varepsilon_{\sigma}(\vec{x}, \vec{u}) = \frac{I_{\sigma}(\vec{x}, \vec{u})}{I_{\sigma, \nu}(\vec{x})} \quad (13)$$

where $I_{\sigma}(\vec{x}, \vec{u})$ is the spectral radiative intensity at the position of the detector in the direction of detection.

In Figure 11, pure alumina sample (with no porosity) is considered in order to validate the Null-Collision algorithm in a simple test-case without scattering. The spectral emission factor predicted with our code for three different temperatures is compared with the one computed with the software FOCUS (Focus, 2016). The input data in our code are the complex refractive indexes for the following temperatures (626 K, 870K and 1023K) for alumina provided by the CEMTHI (Meneses et al., 2006)

The results obtained are merged with those of FOCUS which ensures that our model works well in this configuration (no scattering).

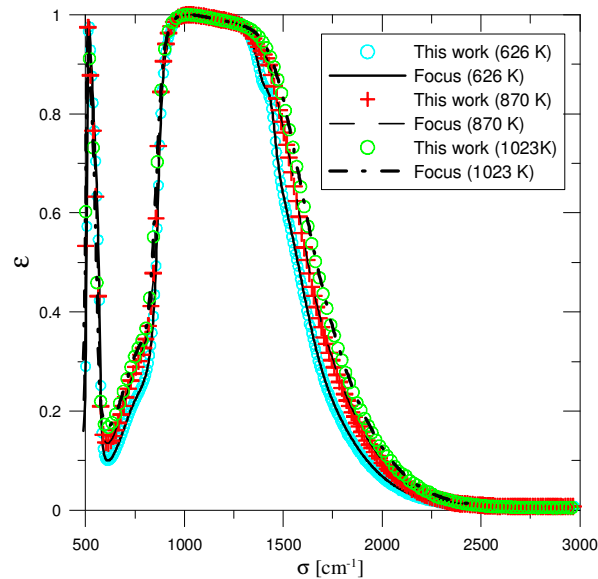


Figure 11. Spectral normal Emission Factor for sample of pure Alumina without porosity (Al_2O_3)

In Figures 12 and 13, a sample of porous alumina ceramic is considered. Porosity implies now that scattering (modeled in our code by the Mie theory) occurs.

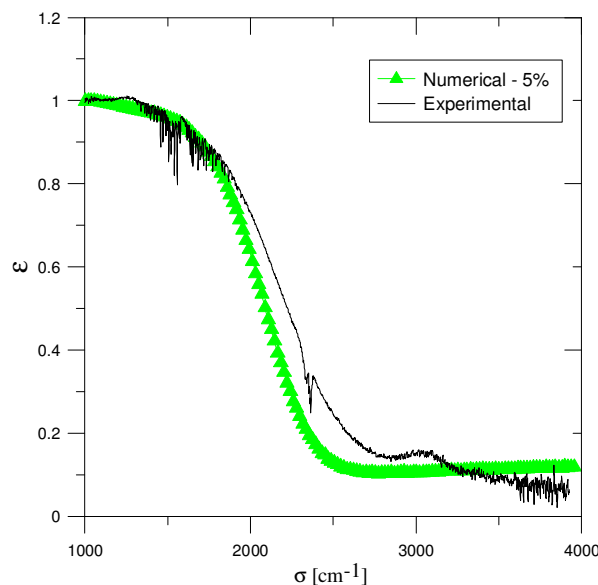


Figure 12. Spectral normal emission factor: Alumina (5% porosity) at $T=820K$

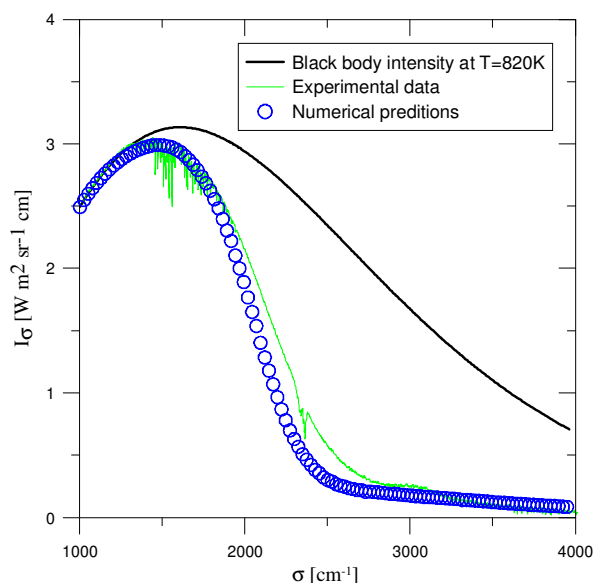


Figure 13. Radiative intensity

In this work, a monodisperse spherical pores of radius $10\mu\text{m}$ is assumed. It can be seen in those figures that experimental and numerical results are very close in a large spectral band. A difference remains significant between 2000 and 3000 cm^{-1} . This difference can be explained by various factors. First, in our code, the sample is considered isothermal which is not exactly the case of the experimental configuration.. Second, various assumptions have been made such as a uniform radius value of the pore, which may not be valid in the studied sample. Moreover, the porosity of the sample was unknown.

Nevertheless, the results are very satisfactory and display a good behavior of the chosen models and the numerical code in porous media in those test - cases. Others samples will also be studied in a close future.

6. CONCLUSION

A Monte Carlo - Null Collision algorithm is presented in this work for the prediction of radiative intensity in heterogeneous material. The code solves the Radiative Transfer Equation (RTE) along with Mie Theory for calculating the radiative properties. The main innovative point of this work is that no homogenization model is required for the determination of macroscopic radiative properties. The developed code treats the different media through a statistical description using the Monte Carlo integration for these simulations. The test case presented in this work refers to a porous sample of alumina, but the numerical code is also able to predict radiative transfer in gaseous media with spherical particle. Current work is in progress to extend the proposed approach to fibrous media.

The first results show that the numerical predictions are very close to the experimental data. The difference noted between the numerical and experimental data may result from various assumptions that will be improved in future works. Assumptions such as polydisperse distribution of pores radius, and cylindrical shape for fiber will be introduced, among others.

In future work, one main objective will be to develop an experimental identification method of the radiative properties. An inverse method will be applied to identify the unknown properties (such as the complex refractive index, or the absorption and scattering coefficients, and the phase function parameters). The coupling of radiative transfer with others heat transfer modes will also be envisaged in those heterogeneous high-temperature semi-transparent media in order to simulate heat transfer in anisothermal heterogeneous media.

7. ACKNOWLEDGMENTS

The authors thank Fapemig and CNPq for their financial support.

8. REFERENCES

Howell J.R., Siegel R. and Mengüç M.P., 2011 Thermal Radiation Heat Transfer, 5th Edition, , CRC Press

- Sacadura J.F., 2011 Thermal radiative properties of complex media: Theoretical prediction versus experimental identification. *Heat Transfer Engineering*. 320, pp. 754-770
- Lefoll S., André F., Delmas A., Bouilly J.M., Aspa Y, 2012. "Radiative transfer modeling inside thermal protection system using hybrid homogenization method for a backward Monte Carlo method coupled with Mie theory", *Journal Phys.: Conference Series* 369
- Taine J., Bellet F., Leroy V., Iacona E., 2010, "Generalized radiative transfer equation for porous medium upscaling: Application to the radiative Fourier law". *Int. J. Heat Mass Transf.* 53, pp. 4071-4081
- Zarrouati M., Enguehard F., Taine J. 2015, "Radiative transfer within strongly non homogenous porous media : Application to a slab of packed particles". *Int. J. Heat Mass Transf.* 91, pp. 936-947
- Petrasch J., Haussener S., Lipinski W., 2011. "Discrete vs. continuum-scale simulation of radiative transfer in semitransparent two-phase media", *J. Quantitative Spectrosc. Radiative Transf.* 112, pp. 1450-1459
- Galtier M., Blanco S., Caliot C., Coustet C., Dauchet J., El Hafi M., Eymet V., Fournier R., Khuong A, Gautrais J., Piaud B, and Terrée G., 2013 "Integral formulation of null-collision Monte Carlo algorithms". *J. Quant. Spectrosc. Radiat. Transf.*, 125, pp.57-68
- Galtier M., Blanco S., Dauchet J., el Hafi M., Eymet V., Roger M., Spiesser C. and Terrée G.. 2016. "Radiative transfer and spectroscopic databases: a line-sampling Monte Carlo approach". *J. Quant. Spectrosc. Radiat. Transf.*, 172, pp. 83-97
- Delmas A., Robin-Carrillon L., Oelhoffen F., Lanternier T, 2010. "Experimental and theoretical characterization of emission from ceramics at high-temperature: investigation on stabilized zirconia and alumina", *Int. J. Thermophys.* 31 pp.1092-1110
- FOCUS, 2016. WebSite: <http://crmht.cnrs-orleans.fr/pot/software/focus.html>.
- Meneses D. De Sousa, Malki M., Echegut P., 2006. "Structure and Lattice Dynamics of Binary Lead Silicate Glasses Investigated by Infrared Spectroscopy", *Journal of Non-Crystalline Solids*, v. 352, pp.769-776